IOP PUBLISHING JOURNAL OF PHYSICS A: MATHEMATICAL AND THEORETICAL

J. Phys. A: Math. Theor. **42** (2009) 495205 (9pp) doi:10.1088/1751-8113/42/49/495205

Uniqueness of magnetotomography for fuel cells and fuel cell stacks

H Lustfeld[1], J Hirschfeld[2], M Reißel[3] and B Steffen[4]

[1] Forschungszentrum Juelich, IFF, 52425 Juelich, Germany
[2] Forschungszentrum Juelich, IAS, 52425 Juelich, Germany
[3] Fachhochschule Aachen, Campus Jülich, 52428 Jülich, Germany
[4] Forschungszentrum Jülich, JSC, 52425 Jülich, Germany

E-mail: h.lustfeld@fz-juelich.de, j.hirschfeld@fz-juelich.de, reissel@fh-aachen.de and b.steffen@fz-juelich.de

Received 17 July 2009, in final form 29 October 2009
Published 25 November 2009
Online at stacks.iop.org/JPhysA/42/495205

Abstract

The criterion for the applicability of any tomographic method is its ability to construct the desired inner structure of a system from external measurements, i.e. to solve the inverse problem. Magnetotomography applied to fuel cells and fuel cell stacks aims at determining the inner current densities from measurements of the external magnetic field. This is an interesting idea since in those systems the inner electric current densities are large, several hundred mA per cm^2 and therefore relatively high external magnetic fields can be expected. Still the question remains how uniquely the inverse problem can be solved. Here we present a proof that by exploiting Maxwell's equations extensively the inverse problem of magnetotomography becomes unique under rather mild assumptions and we show that these assumptions are fulfilled in fuel cells and fuel cell stacks. Moreover, our proof holds true for any other device fulfilling the assumptions listed here. Admittedly, our proof has one caveat: it does not contain an estimate of the precision requirements the measurements need to fulfil for enabling reconstruction of the inner current densities from external magnetic fields.

PACS numbers: 02.30.Zz, 42.30.Wb, 82.47.Ed, 82.47.Gh, 82.47.Lh, 82.47.Nj, 82.47.Pm

(Some figures in this article are in colour only in the electronic version)

1. Introduction

Over the last two decades fuel cells and fuel cell stacks (the arrangement of many fuel cells in series) have attracted much attention [1–6] because their efficiency, not limited by Carnot's

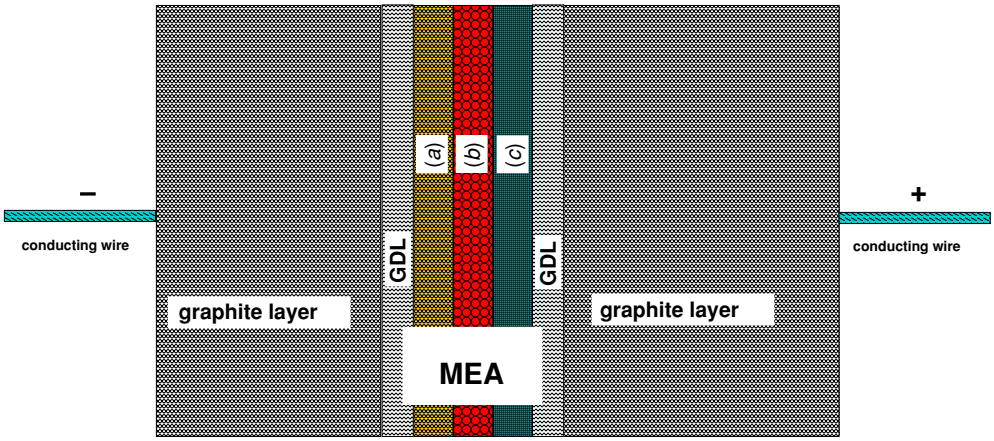

Figure 1. Schematic representation of the MEA in a fuel cell. The MEA consists of two gas diffusion layers (GDL), the catalytic layer at the anode denoted by (*a*), the electrolytic layer denoted by (*b*) and the catalytic layer at the cathode denoted by (*c*). The layers containing the channels for the fuel and the exhaust gas are fabricated, e.g. from graphite. Note that the scales in depth width and height are not identical: typical height is 20 cm, typical depth is 20 cm as well, typical thickness of the layers (*a*), (*b*) and (*c*) is 0.06 mm each, typical thickness of the GDL is 0.2 mm each and the thickness of the graphite layers is 1 mm each or less.

law, can in principle be close to 1. However, they are very complex devices: from a theoretical point of view, since their functioning is still not well understood in detail, and from a practical point of view, since the efficiency of today's fuel cells is far below its theoretical value. Moreover, they tend to become unstable [7, 8].

Under such circumstances good diagnostics is essential. At the same time it is desirable to avoid direct measurements in the inner of these devices, since any local manipulation in the interior may change the internal state. Thus, tomographic methods are favoured and magnetotomography [9] seems to be one option, because the current densities in fuel cells and fuel cell stacks are large: several hundreds mA per cm^2.

It is remarkable that the forward problem of magnetotomography is relatively easy: in fact, if the relative permeability μ is close to 1—which holds true in present day fuel cells—and if external perturbations can be neglected—which is more questionable—then the Biot–Savart operator suffices to obtain a unique solution of the magnetic field from the knowledge of the internal electric current density. The price paid is a huge nullspace when trying to solve the inverse problem just by use of the Biot–Savart operator [10]. This nullspace can be reduced to a certain extent when using further restrictions (cf [11] and references therein). Nevertheless, till today a nullspace remains when trying this ansatz for fuel cells and fuel cell stacks respectively.

This is not surprising. The external magnetic field depends on the current densities $\mathbf{j}$ at any point in the fuel cell (fuel cell stack). But that is not what we really need. We intend much less: the normal component of the current density j_n passing through a so-called membrane electrode assembly (MEA). If we want to proceed successfully, we have to find a connection between j_n and $\mathbf{j}$. This connection is given by Maxwell's equations and Ohm's law—provided we know how an MEA influences the currents in the fuel cell (fuel cell stack). The kind of this influence will be explained below.

The current densities in a fuel cell are well described in the various layers by Ohm's law except in the MEA, cf figure 1. The MEA is the heart of the fuel cell. It contains

two catalytic layers where the catalytic processes take place, and an electrolytic layer, where the ionic transport takes place. To describe all this on a microscopic scale is a formidable task—fortunately, it does not make much sense either as far as magnetotomography is concerned. In fact, it is hopeless to get information from magnetotomography on a microscopic scale [12, 14]. Therefore, a representation for the MEA on a non-microscopic scale is needed which is appropriate, i.e. physically realistic and mathematically well defined. Such a representation has been introduced recently [14, 15] and will be discussed in section 2. This is the preparation for section 3 in which the proof of uniqueness will be given. The further assumptions for and the consequences of this proof will be discussed in the conclusion.

2. Representation of the MEA on a non-microscopic scale

The MEA is composed of two gas diffusion layers (GDLs) constituting its external surfaces. Between those are (a) the catalytic layer at the anode where chemical reactions (e.g. $H_2 \rightarrow 2H^+ + 2e^-$) as well as transport of ions and electrons take place, (b) the electrolytic layer, through which the ions are migrating and (c) the catalytic layer at the cathode where again chemical reactions (e.g. $2H^+ + 1/2O_2 + 2e^- \rightarrow H_2O$) as well as transport of ions and electrons take place. In these three layers Ohm's law is not valid (whereas the current through the GDL can be described by Ohm's law). As is well known from equivalent circuit schemes, it is possible to introduce effective, space dependent conductivities $\sigma(\mathbf{r})$ for these three layers that are treated as parameters and describe the state of the MEA around an operating point [12, 13]. Here we use a different approach. On a non-microscopic scale the state of the MEA is well described by the normal current density $j_n(\mathbf{r})$ going through it. Moreover, the three layers together have a thickness of about 0.2 mm—a scale that is below the resolution magnetotomography can achieve [12, 14]. Therefore, the three layers can be replaced by (i) a boundary layer in the middle of these three layers to which the normal current densities on the MEA now refer to, (ii) two small layers of about 0.1 mm thickness located on both sides of this boundary layer with transverse and longitudinal conductivities obtained from an operating point of the MEA. Because the thickness of these layers is very small, exact values for these conductivities are not required[5].

In this way the real MEA, in which complicated mixed chemical and transport processes occur, has been replaced by an equivalent MEA. Chemical processes do not appear directly and current densities on a microscopic scale, irrelevant for magnetotomography, have disappeared. However, the really important quantity, the normal current density through the MEA surface, has been fully taken into account. Furthermore, the original thickness of the above-mentioned three layers has been included by small layers around a new boundary layer. Both GDLs are fully incorporated in this scheme. We denote the present replacement of the three inner layers of the original MEA by two layers and an internal boundary layer on which the normal current density is well defined, as the *thin MEA approximation* [14, 15].

It should be mentioned that—as in the original MEA—the electric potential is not equal on both sides of the newly constructed boundary layer. This is not only harmless but also quite necessary since it needs power to move currents from one side of the MEA to the other side. This power is provided by the underlying chemical processes.

[5] In reality a focused normal current entering the MEA will have spread when leaving it on the other side. It is a very good choice setting the transverse conductivity in these small layers such that this spreading is taken into account correctly. The longitudinal conductivity is not critical, setting it to the value of the transverse conductivity is one possible option.

Using the thin MEA approximation we have a quite realistic description of an MEA and at the same time a mathematically well-defined structure. It will turn out that the uniqueness of magnetotomography can now be proven for fuel cells and fuel cell stacks. This is shown in the next section.

3. Proof: uniqueness of the inverse problem

The fuel cell and the fuel cell stack respectively consist of an area G_b with certain mathematical properties. These are now listed.

Definition 1. *A 3-dimensional area is denoted as G_b if*

(I) G_b *is connected.*

(II) G_b *can be divided into N connected areas G_i with*[6]

(1)

$$\overset{o}{G}_i \cap \overset{o}{G}_j = \emptyset \qquad \text{for} \quad i \neq j \tag{1}$$

(2) in each G_i the differential equation $-\nabla^2\Phi_i = 0$ with boundary condition $\partial\Phi/\partial n$ (derivative with respect to the outer normal) has (up to a constant) a unique solution in G_i and the surface of G_i is such that Gauss's theorem applies,

(3) in each G_i the conductivity σ_i is constant and the current density **j** *is given by Ohm's law:*

$$\mathbf{j}_i = -\sigma_i \nabla \Phi_i .$$

(III) A permutation $\nu = p(k)$, $1 \leqslant k \leqslant N$, exists with the following.

(1) Given any $1 \leqslant k \leqslant N$ and $\nu = p(k)$, denoting by $S_{\mathrm{tot},\nu}$ the exterior surface of $\cup_{k'=1}^{k} G_{p(k')}$, by S_ν the surface of G_ν and by $S_{\mathrm{part},\nu}$ the surface, given by

$$S_{\mathrm{part},\nu} = S_\nu \cap S_{\mathrm{tot},\nu}, \tag{2}$$

$$S_{\mathrm{part},\nu} \neq \emptyset \tag{3}$$

(2) $\exists$ 3 points $\mathbf{r}_{\nu,i}$, $i = 1, 2, 3$, with the properties

(i)

$$\mathbf{r}_{\nu,i} \in S_{\mathrm{part},\nu}, \qquad i = 1, 2, 3 \tag{4}$$

$\exists$ a neighborhood $U(\mathbf{r}_{\nu,1})$ around $\mathbf{r}_{\nu,1}$ on $S_{\mathrm{part},\nu}$, i.e. $U(\mathbf{r}_{\nu,1}) \subset S_{\mathrm{part},\nu}$ with

$$\mathbf{n}(\mathbf{r}) = \text{const} \quad \textit{for} \quad \mathbf{r} \in U(\mathbf{r}_{\nu,1}). \tag{5}$$

(ii) The same holds true for $\mathbf{r}_{\nu,2}$:

$$\mathbf{n}(\mathbf{r}) = \text{const} \quad \textit{for} \quad \mathbf{r} \in U(\mathbf{r}_{\nu,2}) \tag{6}$$

(iii) $\exists$ a neighborhood $U(\mathbf{r}_{\nu,3})$ around $\mathbf{r}_{\nu,3}$ on $S_{\mathrm{part},\nu}$, i.e. $U(\mathbf{r}_{\nu,3}) \subset S_{\mathrm{part},\nu}$ with

$$\mathbf{n}(\mathbf{r}) = \textit{continuous for} \quad \mathbf{r} \in U(\mathbf{r}_{\nu,3}) \tag{7}$$

(iv) $\mathbf{n}(\mathbf{r}_{\nu,1})$, $\mathbf{n}(\mathbf{r}_{\nu,2})$, $\mathbf{n}(\mathbf{r}_{\nu,3})$ are linear independent of each other.

Note. It might happen that a point, say $\mathbf{r}_{\nu,1}$, is located on a position where two surfaces touch each other. That does not matter here since due to continuity we can find a point $\mathbf{r}'_{\nu,1}$ and an equivalent neighborhood $U'(\mathbf{r}'_{\nu,1}) \subset U(\mathbf{r}_{\nu,1})$ where this does not happen.

[6] In this paper we use the notation: $\overset{o}{X}$ is the interior of X.

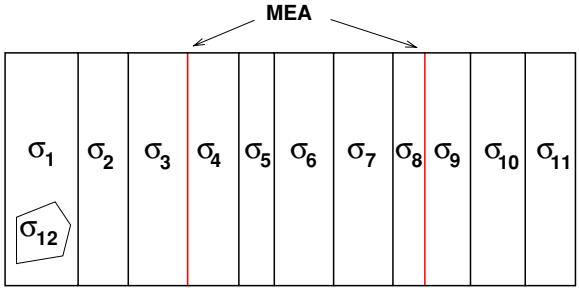

Figure 2. Schematic representation of a fuel cell stack (with 2 MEAs only) build up from 12 connected areas G_i of materials with different conductivities. One possible permutation is $p(1) = 12$, $p(2) = 1$, $p(3) = 2$, $p(4) = 3$, etc. G_b fulfills all requirements of definition 1.

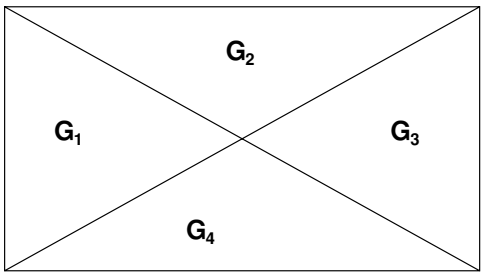

Figure 3. A rectangle consisting of 2D triangles G_i with different conductivities σ_i each. All G_i have one 1D external surface only. In 3D this becomes a cuboid, consisting of 3D G_i with only three external surfaces. Property III,2,iv of definition 1 is not fulfilled, because the three unit normals are linear dependent. Therefore, according to that definition this cuboid is not an area of type G_b. However, this would be quite different if, e.g. the upper surface in G_3 would be arched. Then this modified cuboid would be an area of type G_b and the permutation p would be $p(1) = 2$, $p(2) = 1$, $p(3) = 4$, $p(4) = 3$.

Examples. *An example for an area G_b of a fuel cell stack fulfilling the assumptions I–III of definition 1 is presented in figure 2. An example of an area fulfilling assumptions I and II, but not III, is shown in figure 3. Fuel cells and fuel cell stacks always fulfill conditions I–III.*

We now give the proof of the following theorem.

Theorem 1. *If an area has the properties*

(a) it is of type G_b, i.e. it has the properties given in definition 1,
(b) its relative permeability $\mu = 1$
(c) all conductivities in the G_i, σ_i, are scalars and $0 \leqslant \sigma < \infty$

then magnetotomography is unique.

Proof. The proof is given by contradiction: let us assume that magnetotomography is not unique. This means that there are two solutions Φ_1 and Φ_2 with different current densities in G_b but with the same *external* currents and the same *external* magnetic field. We consider the properties of

$$\Phi_D = \Phi^{(1)} - \Phi^{(2)}. \tag{8}$$

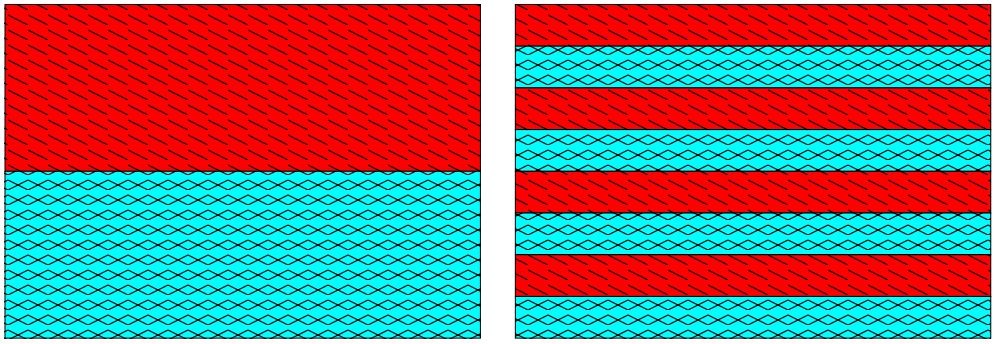

Figure 4. A layer with different longitudinal $\sigma_\parallel$ and transverse $\sigma_\perp$ conductivity can be approximated by two layers with scalar conductivities σ_1 and σ_2 fulfilling the equations $\sigma_1 + \sigma_2 = 2\sigma_\perp$ and $1/\sigma_1 + 1/\sigma_2 = 2/\sigma_\parallel$, cf (a). The approximation becomes much better if not just one layer but M thinner layers of the same two materials with (scalar) conductivities as before are taken, cf (b). The magnetic field $\mathbf{H}$ converges for $M \to \infty$ to the magnetic field of the layer with $\sigma_\parallel \neq \sigma_\perp$.

Its magnetic field $\mathbf{H}_D$ is not due to external currents. This property together with $\mu = 1$ means that the magnetic field $\mathbf{H}_D$ is generated *exactly* by the vector potential of Biot–Savart:

$$\mathbf{A}_D(\mathbf{r}) = \frac{1}{4\pi} \int_{G_b} \mathrm{d}^3 r' \frac{1}{|\mathbf{r} - \mathbf{r}'|} \mathbf{j}_D(\mathbf{r}') \tag{9}$$

where $\mathbf{A}_D$ is the vector potential of $\mathbf{H}_D$ and $\mathbf{j}_D$ is obtained from

$$\mathbf{j}_D = -\sigma_i \nabla \Phi_D \quad \text{in } G_i. \tag{10}$$

This can be written as

$$\begin{aligned} &\mathbf{A}_D(\mathbf{r}) = \mathbf{A}_1(\mathbf{r}) + \nabla W(\mathbf{r}) \\ &\text{with} \\ &\mathbf{A}_1(\mathbf{r}) = \frac{1}{4\pi} \sum_i \int_{G_i} \mathrm{d}^3 r' \, \nabla' \left[\frac{-1}{|\mathbf{r} - \mathbf{r}'|} \sigma_i \Phi_D(\mathbf{r}') \right] \\ &W(\mathbf{r}) = \frac{1}{4\pi} \sum_i \int_{G_i} \mathrm{d}^3 r' \, \sigma_i \Phi_D(\mathbf{r}') \frac{-1}{|\mathbf{r} - \mathbf{r}'|}. \end{aligned} \tag{11}$$

∇W does not contribute to the magnetic field. Therefore, the magnetic field is obtained from $\mathbf{A}_1$ alone. We transform the volume-integral in the formula for $\mathbf{A}_1$ by partial integration into surface integrals. Of course, all the external surfaces as well as all internal boundary layers between the G_i have to be taken into account[7]. Partial integration leads to

$$\mathbf{A}_1 = \frac{1}{4\pi} \sum_{(i,j)} \int_{F_{(i,j)}} \mathrm{d}s \, \mathbf{n}_{(i,j)}(\mathbf{r}') \frac{-1}{|\mathbf{r} - \mathbf{r}'|} [\sigma_i \Phi_{Di}(\mathbf{r}') - \sigma_j \Phi_{Dj}(\mathbf{r}')]. \tag{12}$$

$F_{(i,j)}$ denotes the boundary area between G_i and G_j. The summation index (i, j) refers to a sum over all inner boundary layers and the outer surface. The outer side of the outer surface gets the index $j = 0$; thus equation (12) is well defined by setting $\Phi_{D,j=0} = 0$.

[7] Note that the MEAs lead to the following effect: consider a boundary layer $F_{(i,j)}$ (with unit normal $\mathbf{n}_{(i,j)}$) separating G_i from G_j. Then the potential Φ_{Di} of G_i may be different from Φ_{Dj} of G_j on the boundary layer $F_{i,j}$.

Now it is clear that $\mathbf{A}_1$ and therefore the magnetic field $\mathbf{H}_D$ are analytic in each $\overset{o}{G}_i$. Next we use property III,2,i of definition 1. Let $\nu = p(N)$. Then on the surface $S_{\text{part},\nu}$ there is a point $\mathbf{r}_{\nu,1}$ and a corresponding unit normal $\mathbf{n}(\mathbf{r}_{\nu,1})$. First, let us assume that $\mathbf{n}(\mathbf{r}_{\nu,1})$ points in the z-direction. This means that the integral for $\mathbf{A}_{1,x}$ and $\mathbf{A}_{1,y}$ has no contribution from a neighbourhood $U(\mathbf{r}_{\nu,1})$. But $\mathbf{A}_1$ is analytic in the exterior of G_b and in G_ν. Therefore, $\exists$ a (3D) ball with finite radius ϵ, $K_\epsilon(\mathbf{r}_{\nu,1})$ in which both, $\mathbf{A}_{1,x}$ and $\mathbf{A}_{1,y}$, are analytic. Therefore, H_{Dz} must be analytic in $K_\epsilon(\mathbf{r}_{\nu,1})$ as well. Therefore, we can continue H_{Dz} analytically from the exterior of G_b into G_ν. Since $H_{Dz} = 0$ in the exterior, it must vanish in $\overset{o}{G}_\nu$.

The generalization is clear: the component of $\mathbf{H}_D$ along $\mathbf{n}(\mathbf{r}_{\nu,1})$ vanishes in G_ν. Because of property III,2,ii the same holds true for the component of $\mathbf{H}_D$ along $\mathbf{n}(\mathbf{r}_{\nu,2})$. Next we exploit property III,2,iii: we construct a line through the point $\mathbf{r}_{\nu,3}$ with the tangent vector given by the cross-product

$$\mathbf{b}_\nu = \mathbf{n}(\mathbf{r}_{\nu,1}) \times \mathbf{n}(\mathbf{r}_{\nu,2}). \tag{13}$$

Because of property III,2,iv $\mathbf{b}_\nu$ cannot vanish. For the same reason the projection of $\mathbf{b}_\nu$ onto $\mathbf{n}(\mathbf{r}_{\nu,3})$ cannot vanish either. Therefore, we can parametrize the equation for the line and $\exists\, \epsilon$

$$\mathbf{r}_{\text{line}}(t) = \mathbf{r}_{\nu,3} + t\mathbf{b}_\nu, \qquad t \text{ real} \tag{14}$$

such that $\mathbf{r}(t) \in G_\nu$ for $0 < t < \epsilon$. We take this line as the axis of a cylinder $c(2t, \eta)$ with length $0 < 2t < 2\epsilon$, whose centre is located at $\mathbf{r}_{\nu,3}$. Because of continuity (cf (7)) there is a diameter $\eta > 0$ of the cylinder such that it penetrates exclusively into G_ν, i.e.

$$c(2t, \eta) \cap (G_b \setminus G_\nu) = \emptyset \qquad \text{for} \quad t < \epsilon. \tag{15}$$

We calculate the integral over the surface of the cylinder, $F_{c(2t,\eta)}$. It follows from $\nabla \mathbf{B}_D = 0$ and $\mu = 1$

$$I(2t, \eta) = 0 = \int_{F_{c(2t,\eta)}} \mathbf{n} \cdot \mathbf{H}_D \, \mathrm{d}s. \tag{16}$$

But $\mathbf{H}_D = 0$ outside G_b; the normal components of $\mathbf{H}_D$ vanish on the cylinder side by construction. Therefore, the integral over the top surface of the cylinder has to vanish as well. Since η can become arbitrarily small, this is only possible if $\mathbf{H}_D(\mathbf{r}_{\text{line}}(t)) \cdot \mathbf{b}_\nu$ vanishes for $0 < t < \epsilon$. Because of continuity, we can repeat the procedure after slightly moving $\mathbf{r}_{\nu,3}$ along $S_{\text{part},\nu}$. Thus, we can prove that there must be a ball $K_\epsilon(\mathbf{r}_0) \subset G_\nu$ with $\mathbf{H}_D(\mathbf{r}) \cdot \mathbf{b}_\nu = 0$ for $\mathbf{r} \in K_\epsilon(\mathbf{r}_0)$. Because $\mathbf{H}_D$ is analytic in $\overset{o}{G}_\nu$, it means that

$$\mathbf{H}_D = 0 \quad \text{in} \ \overset{o}{G}_{p(N)}. \tag{17}$$

Because of property III in definition 1 we can continue with the same arguments and show that

$$\mathbf{H}_D = 0 \quad \text{in} \ \overset{o}{G}_{p(N-1)}. \tag{18}$$

Repeating this procedure we have[8]

$$\mathbf{H}_D(\mathbf{r}) \equiv 0. \tag{19}$$

Because of $\nabla \times \mathbf{H}_D = \mathbf{j}_D$ all electric currents are zero in contradiction to the assumption. This ends the proof. □

[8] At first we have the restriction that $\mathbf{H}_D$ could be nonzero on the internal boundary layers and the external surface of G_b. But it is not possible that a finite electric current exists on 2D areas in G_b due to assumption (c) of theorem 1. Then taking the integral form of $\nabla \times \mathbf{H}_D = 0$ and $\nabla \mathbf{H}_D = 0$ leads to the conclusion that $\mathbf{H}_D$ has to vanish everywhere.

In real fuel cells and fuel cell stacks some materials, in particular graphite, are being used in which longitudinal and transverse conductivities are different. Then the conductivity is no longer a scalar but a matrix, albeit a simple one: the matrix is diagonal, the first element in the diagonal is different from the other two. Generalizing the previous argument to this case is nearly trivial. The reason is that two adjacent layers with different (scalar) conductivities can simulate this situation, cf figure 4. Now if an electric current could appear in the solution of Φ_D in case the longitudinal conductivity $\sigma_\parallel$ is different from the transverse one, $\sigma_\perp$, this could be simulated by M small layers of two kinds put alternately together. The (external and internal) magnetic field $\mathbf{H}$ (obtained from the Biot–Savart integral) would converge in the limit $M \to \infty$ and therefore an internal magnetic field had to appear already at finite M. But then application of theorem 1 would be possible and would again lead to a contradiction. Therefore, magnetotomography is unique even in the case that longitudinal and transverse conductivities are different in the materials.

4. Conclusion

In this paper we have shown that by use of magnetotomography the internal electric current densities of fuel cells and fuel cell stacks can be determined uniquely. The assumptions are rather mild:

(A) The cells must consist of nonmagnetic and nonparamagnetic material. In other words, the relative permeability μ must be close to 1. That is fulfilled in the fuel cells being used at present. And as far as we know there is no urgent necessity of changing this in the future.

(B) The proof rests on the assumption that the real MEA can be replaced by another one that avoids taking into account the very complex chemical and physical processes and currents occurring on a micro scale. We think that our approximation of the MEA (we call it the thin MEA approximation) is realistic and at the same time avoids those small scales. This feature is advantageous because magnetotomography is unable to resolve processes taking place on a very fine scale [12, 14] anyway.

A disadvantage of our proof is a practical one: there is no estimate in the proof how precise magnetic fields have to be determined. We believe that a final answer to this question can only be found numerically; estimates for fuel cells have been worked out already [12, 14]. Estimates for fuel cell stacks are in progress.

We would like to point out that our proof is not restricted to fuel cells and fuel cell stacks but is valid for any areas having the properties listed in definition 1.

References

[1] Appleby A J and Foulkes F R 1988 *Fuel Cell Handbook* (New York: van Nostrand Reinhold)
[2] Heinzel A, Nolte R, Ledjeff-Hey K and Zedda M 1998 Membrane fuel cells—concepts and system design *Electrochim. Acta* **43** 3817–20
[3] Scott K, Taama W M and Argyropoulos P 1999 Engineering aspects of the direct methanol fuel cell system *J. Power Sources* **79** 43–59
[4] McLean G F, Niet T, Prince-Richard S and Djilali N 2002 An assessment of alkaline fuel cell technology *Int. J. Hydrogen Energy* **27** 507–26
[5] Dohle H, Schmitz H, Bewer T, Mergel J and Stolten D 2002 Development of a compact 500 W class direct methanol fuel cell stack *J. Power Sources* **106** 313–22
[6] Wang L, Husar A, Zhou T and Liu H 2003 A parametric study of PEM fuel cell performances *Int. J. Hydrogen Energy* **28** 1263–72
[7] Yoon Y G, Lee W Y, Yang T H, Park G G and Kim C S 2003 Current distribution in a single cell of PEMFC *J. Power Sources* **118** 193–9

[8] Noponen M, Mennoloa T, Mikkola M, Hottinen T and Curnd P 2002 Measurement of current distribution in a free-breathing PEMFC *J. Power Sources* **106** 304–12
[9] Hauer K H, Potthast R, Wüster T and Stolten D 2005 Magnetotomography—a new method for analysing fuel cell performance and quality *J. Power Sources* **143** 67–74
[10] Kress R, Kühn L and Potthast R 2002 The reconstruction of a current distribution from its magnetic field *Inverse Problems* **18** 1127–46
[11] Potthast R and Wannert M 2009 Uniqueness of current reconstructions for magnetic tomography in multi-layer devices *SIAM J. Appl. Math.* **70** 563–78
[12] Lustfeld H, Reißel M, Schmidt U and Steffen B 2009 Reconstruction of electric currents in a fuel cell by magnetic field measurements *J. Fuel Cell Sci. Technol.* **6** 021012
[13] More detailed results are presented in: Schmidt U 2007 *Numerische Sensitivitätsanalyse für ein Tomographieproblem bei Brennstoffzellen* (Diploma Thesis), Fachhochschule Aachen, Abteilung Jülich (Jülich)
[14] Lustfeld H, Reißel M and Steffen B 2009 Magnetotomography and electric currents in a fuel cell *Fuel Cells* **9** 474
[15] Hirschfeld J 2009 Tomographic problems in the diagnostics of fuel cell stacks *Diploma Thesis* Jül-Report Jül-4291 Forschungszentrum Jülich, Jülich http://hdl.handle.net/2128/3588